

Electronic Supporting Information

Rational Design on Conjugated Side Chains for High Performance All Polymer Solar Cells

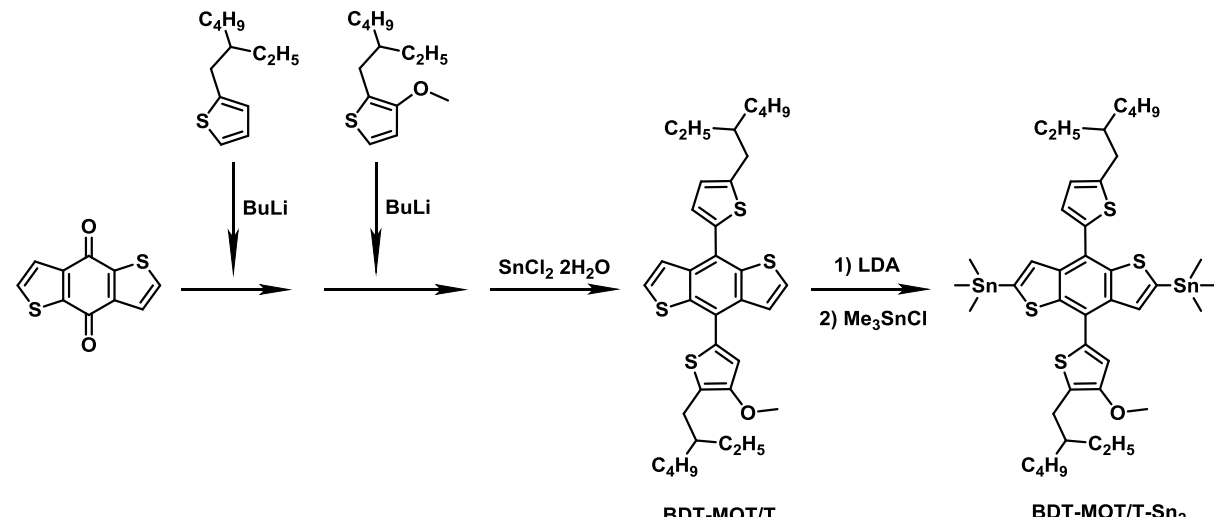
Wei Huang,^{‡,a} Meilin Li,^{‡,a} Fengyuan Lin,^{‡,a} Yang Wu,^b Zhifan Ke,^b Xing Zhang,^a Rui Ma,^a Tingbin Yang,^a Wei Ma^{*b} and Yongye Liang^{*a}

^a Department of Materials Science and Engineering, Shenzhen Key Laboratory of Printed Electronics, South University of Science and Technology of China, Shenzhen 518055, P. R. China. E-mail: liangyy@sustc.edu.cn

^b State Key Laboratory for Mechanical Behavior of Materials, Xi'an Jiaotong University, Xi'an 710049, PR China. E-mail: msewma@xjtu.edu.cn

[‡] These authors contributed equally to this work.

1. Supplementary scheme and figures



Scheme S1. Schematic diagram of BDT-MOT/T organotin monomer.

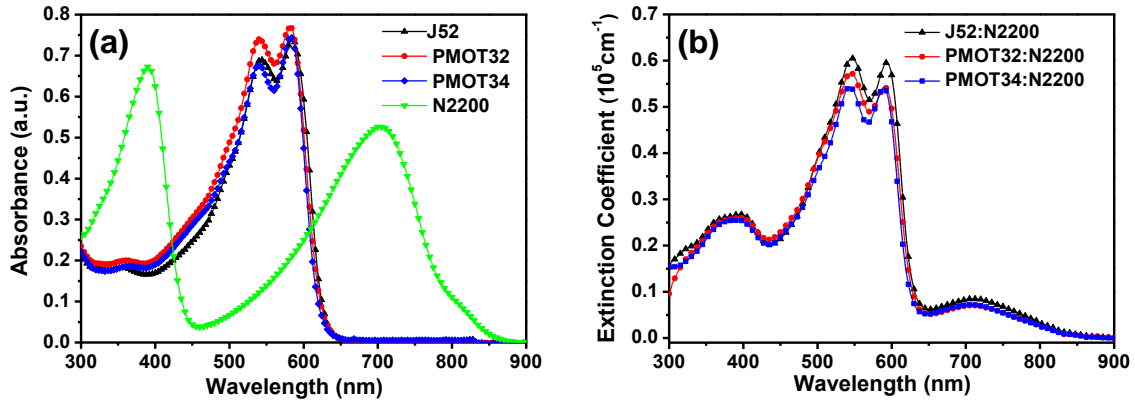


Fig. S1 (a) UV-Vis absorbance of dilute polymer solutions in CF (0.01mg/ml for J52, PMOT32, PMOT34 and 0.02mg/ml for N2200) (b) UV-Vis absorption of three polymer blends processed from CF with 0.7% DIO followed by thermal annealing.

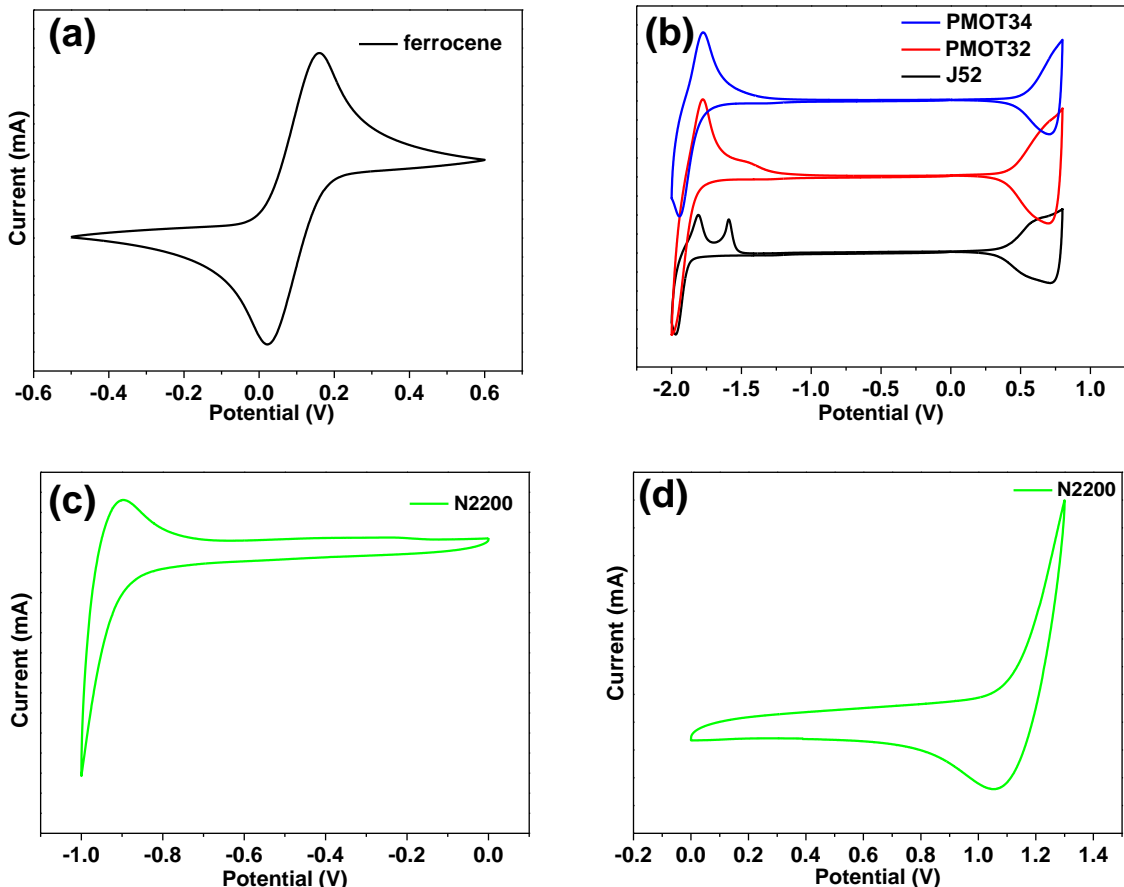


Fig. S2 Cyclic voltammetry curves of the internal reference ferrocene (a), three p-type polymers (b), and N2200 under the reduction(c) and oxidation (d) potential.

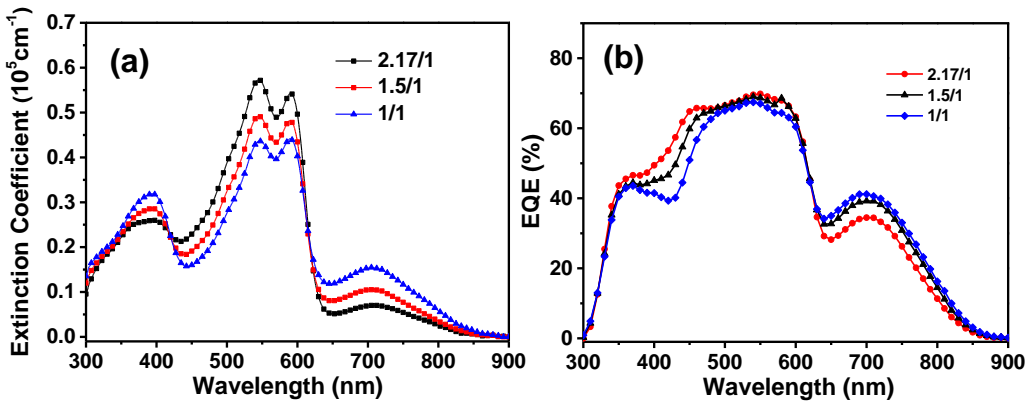


Fig. S3 (a) UV-Vis absorbance of PMOT32:N2200 blend films in different D/A ratios processed from CF+0.7%DIO. (b) EQE spectra of the corresponding champion devices in PMOT32:N2200 solar cells fabricated from different D/A ratios under AM1.5G solar radiation.

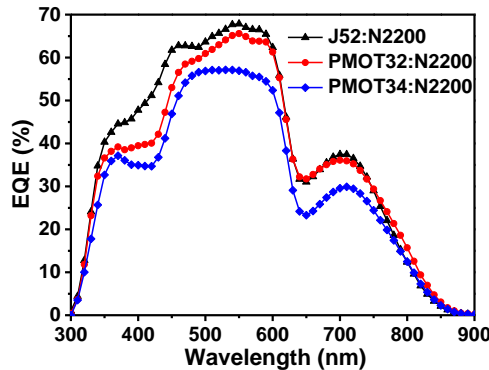


Fig. S4 EQE spectra of the corresponding champion devices in the polymer:N2200 solar cells fabricated from *o*-xylene with 1% DIO under AM1.5G solar radiation.

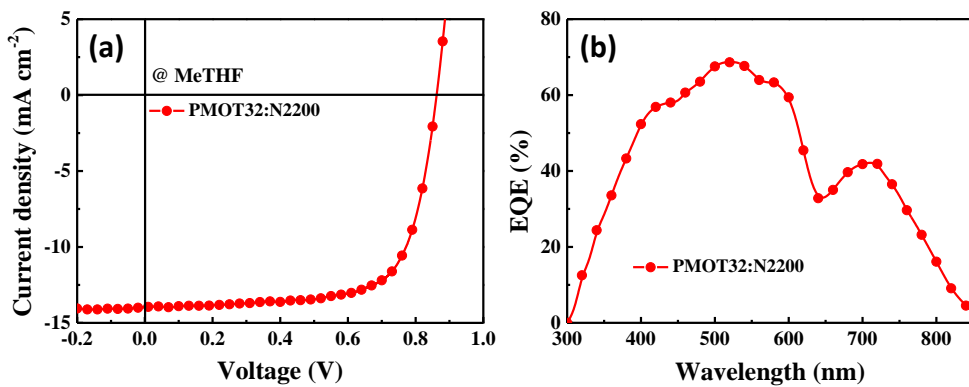


Fig. S5 (a) The J-V characteristics of the PMOT32:N2200 solar cells fabricated from MeTHF under AM1.5G solar radiation and (b) EQE spectra of the corresponding devices in (a).

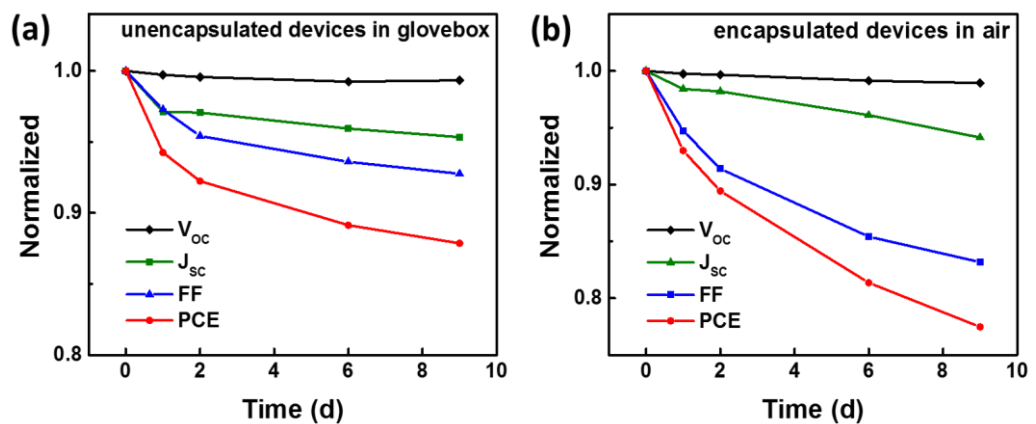


Fig. S6 Normalized stability of (a) unencapsulated devices in glovebox, and (b) encapsulated devices in air of 20°C and 50% humidity.

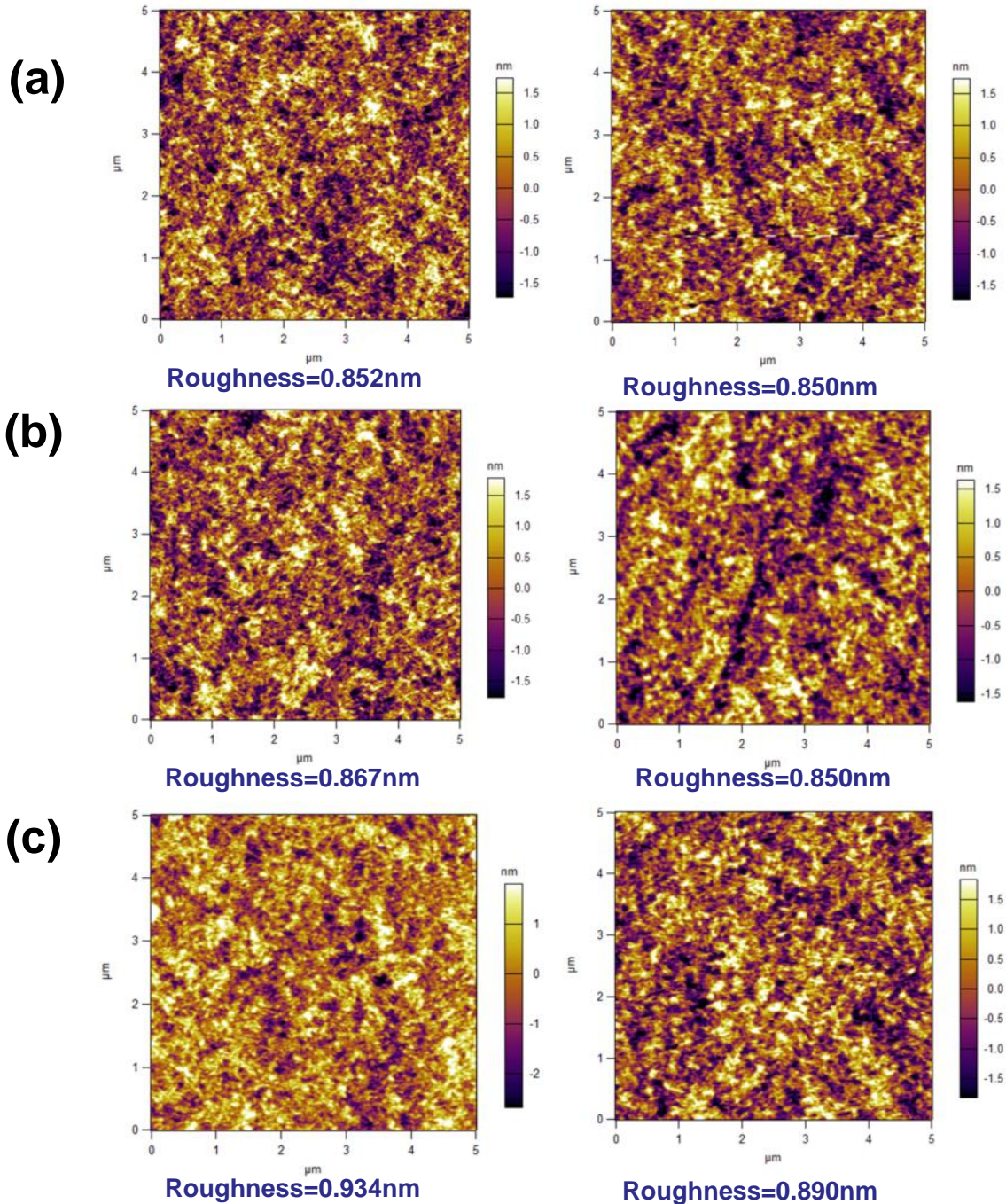


Fig. S7 AFM topography images of three blends without thermal annealing on the left and with TA on the right, (a) for J52:N2200, (b) for PMOT32:N2200 and (c) for PMOT34:N2200, respectively. The root mean square (RMS) roughness is listed below the corresponding image.

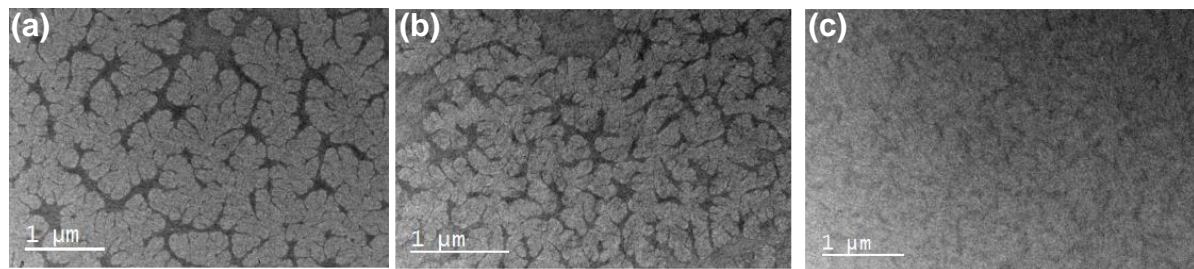


Fig. S8 TEM images of (a) J52:N2200, (b) PMOT32:N2200 and (c) PMOT34:N2200 blends processed from *o*-xylene with 1% DIO after thermal annealing.

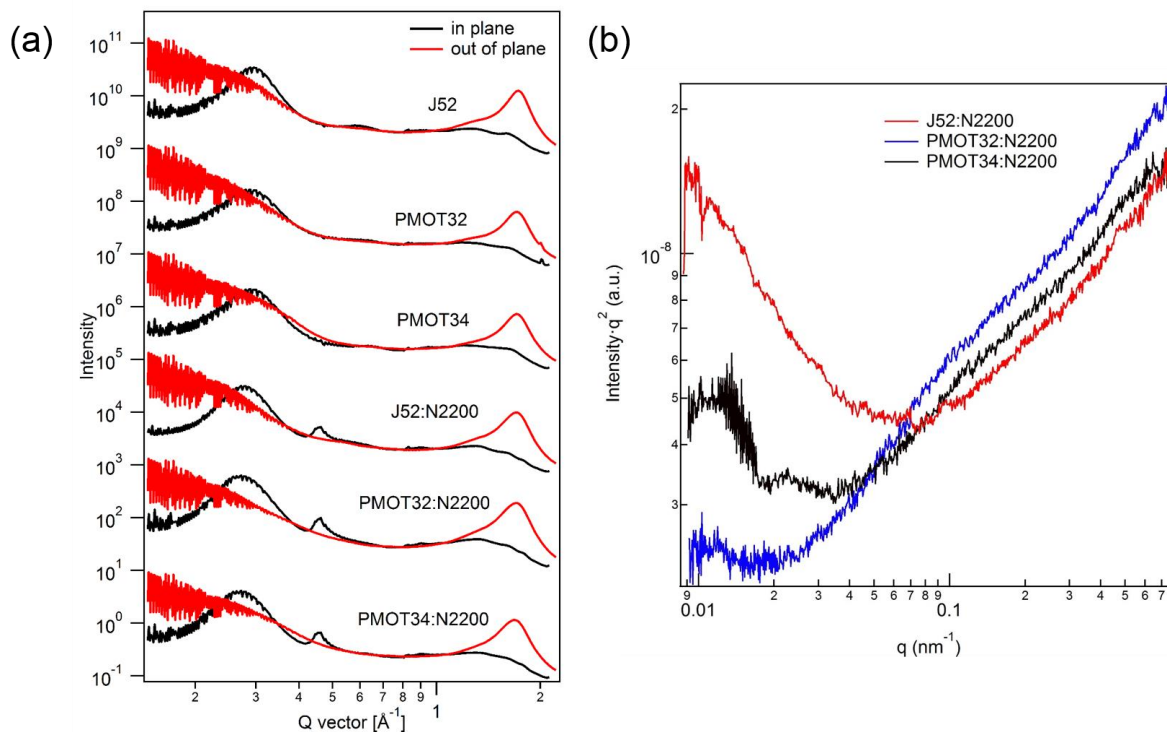


Fig. S9 (a) Scattering profiles in plane and out of plane for three pristine and corresponding blends with N2200. (b) RSoXS plots of the three polymer blends.

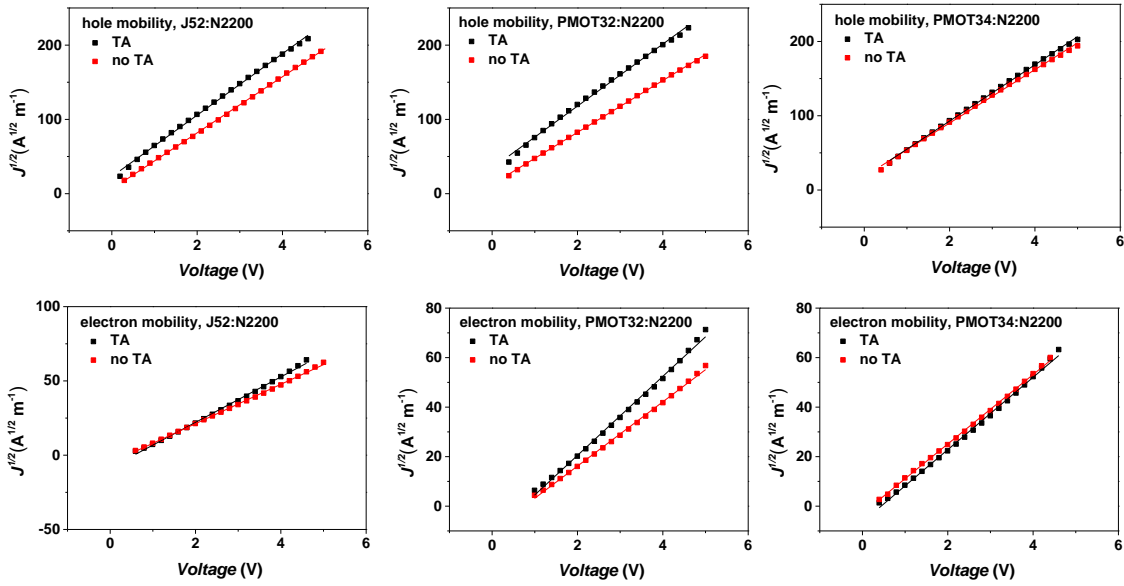


Fig. S10 $J^{1/2}$ - V plots of hole-only (a) and electron-only (b) architectures for three different blend films based on Space-charge-limited current (SCLC) model.

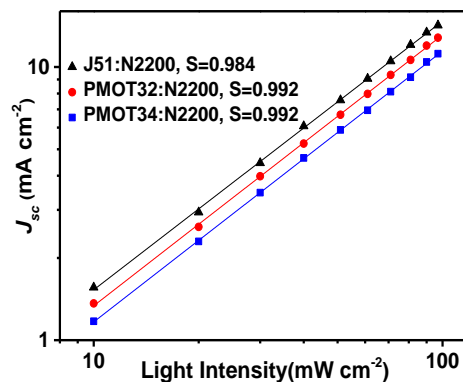


Fig. S11 J_{sc} versus light intensity plots of the blend films based on the equation: $J_{sc} \propto P^S$, P stands for the light intensity and S for the slope of the corresponding fitting curve, which is indicated in the figure.

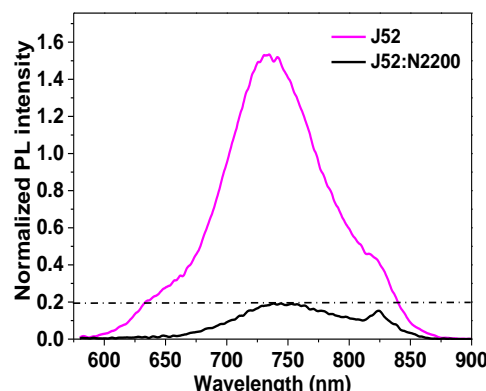


Fig. S12 Normalized photoluminescence (PL) spectra of pristine polymer J52 and blend film with N2200 when excited at the wavelength of 545nm.

2. Supplementary tables

Table S1. Optical and physical properties of the polymers involved in this work.

Polymers	Film $\lambda_{\text{max}}/\text{nm}$	Film $\lambda_{\text{edge}}/\text{nm}$	$E_g^{\text{opt}}/\text{eV}$	EA /eV	IP /eV	M_n/kDa	PDI
J52	546,593	631	1.96	3.16	5.10	31.4	1.79
PMOT32	545,590	629	1.97	3.22	5.14	38.5	2.16
PMOT34	542,588	624	1.99	3.33	5.26	32.8	1.91
N2200	392,700	851	1.46	3.79	5.84	120.6	1.52

Table S2. Photovoltaic performance of PMOT32:N2200 (CF+0.7% DIO) based all-PSCs with different D/A ratio under the illumination of AM1.5G, 100 mW cm⁻².

D/A (wt/wt)	V_{oc} (V)	J_{sc} (mA cm ⁻²)	FF (%)	PCE (%)
1/1	0.852	14.16	54.70	6.60
1.5/1	0.861	14.05	62.64	7.58
2.17/1	0.869	13.86	70.68	8.52
2.7/1	0.863	13.04	67.05	7.55

Table S3. Photovoltaic performance of donor polymer: N2200 (2.17/1, wt/wt, CF+0.7%DIO) based all-PSCs with/without thermal annealing (TA).

Polymer blends	condition	V_{oc} (V)	J_{sc} (mA cm ⁻²)	FF (%)	PCE (%)
J52:N2200	TA	0.798	14.05	67.0	7.51
	no	0.796	13.34	64.2	6.82
PMOT32:N2200	TA	0.869	13.86	70.7	8.52
	no	0.870	13.15	67.3	7.71
PMOT34:N2200	TA	0.912	11.83	67.2	7.25
	no	0.911	11.46	66.1	6.90

Table S4. Photovoltaic performance of J52:N2200, PMOT32:N2200 and PMOT34:N2200 (2.17/1, wt/wt, CF+0.7% DIO) with different thicknesses.

Polymer blends	Thickness (nm)	V _{oc} (V)	J _{sc} (mA cm ⁻²)	FF (%)	PCE (%)
J52: N2200	90	0.797	13.20	66.8	7.03
	110	0.798	14.05	67.0	7.51
	140	0.792	14.10	65.0	7.25
	180	0.788	13.56	57.2	6.11
	250	0.769	13.10	49.6	5.00
PMOT32:N2200	90	0.863	11.35	70.3	6.89
	105	0.865	13.64	68.0	8.02
	125	0.869	13.86	70.7	8.52
	160	0.862	13.74	66.9	7.91
	200	0.852	13.59	59.6	6.90
	250	0.845	12.72	54.1	5.82
	285	0.848	12.32	49.9	5.22
	100	0.910	10.56	66.7	6.41
PMOT34:N2200	130	0.912	11.83	67.2	7.25
	180	0.902	10.65	59.8	5.74
	255	0.892	9.42	48.5	4.07

Table S5. Summary of mobility for three different polymer blends.

Polymer blends	μ_h (cm ² V ⁻¹ s ⁻¹)		μ_e (cm ² V ⁻¹ s ⁻¹)	
	No TA	TA	No TA	TA
J52:N2200	8.64×10^{-4}	9.92×10^{-4}	2.63×10^{-4}	3.82×10^{-4}
PMOT32:N2200	7.94×10^{-4}	8.86×10^{-4}	2.60×10^{-4}	3.75×10^{-4}
PMOT34:N2200	8.26×10^{-4}	8.84×10^{-4}	2.51×10^{-4}	2.87×10^{-4}

Table S6. Summary of J_{sat} , calculated G_{max} and $P(E, T)$ for three different polymer blends.

Polymer blends	J _{sat} (mA cm ⁻²)	G _{max} (m ⁻³ S ⁻¹)	P (E, T) (%)
J52:N2200	15.57	8.39×10^{27}	0.914
PMOT32:N2200	15.41	8.23×10^{27}	0.896
PMOT34:N2200	14.19	7.39×10^{27}	0.830

3. Further discussion on the cost of active materials

The acceptor material, N2200 is widely used as n-type semiconducting material and has been commercialized by many companies. The donor material, PMOT32, is synthesized from the BTD and FTAZ monomers. The synthesis of PMOT32 can be less complicated than the well-known donor polymer PTB7-TH, which is sold in around \$750/g now. We believe that further scale-up and synthesis optimization could make these materials with acceptable cost.